

# Project 1 - SI1336 Simulation and Modelling Oscillations and Chaos

Raymond Wang

November 5, 2020

# Project 1.1

The solutions for the position,  $\theta(t)$  and velocity,  $\dot{\theta}(t)$  comparisons were derived using Velocity Verlet integration. As will be shown later, this is primarily attributed to its satisfactory energy-preserving characteristics in comparison with the other methods. Initial conditions  $\theta(0)/\pi = 0.1, 0.3, 0.5$  and  $\dot{\theta}(0) = 0$ , in addition to a step size of  $\Delta t = 0.01$  were utilized.

## Comparisons for the harmonic oscillator

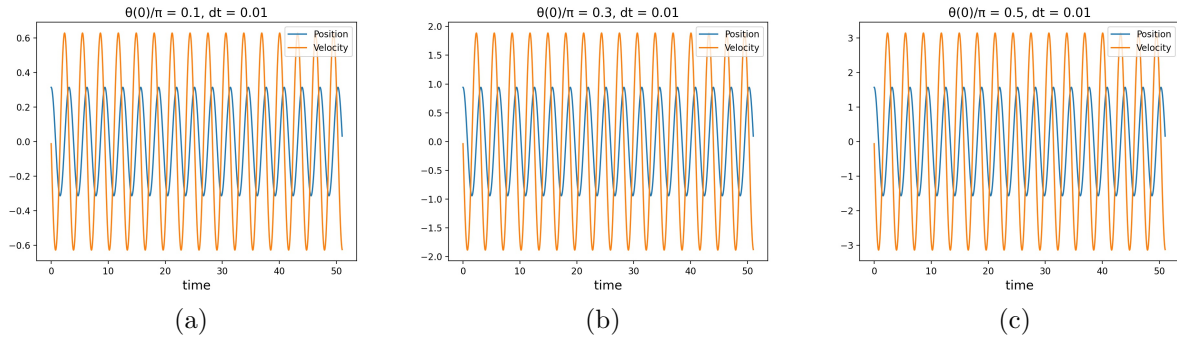


Figure 1: (a)  $\theta(0)/\pi = 0.1$ ; (b)  $\theta(0)/\pi = 0.3$ ; (c)  $\theta(0)/\pi = 0.5$

As can be noted, greater initial angle yields an increase in amplitude for the numerically simulated oscillations.

## Comparisons for the pendulum

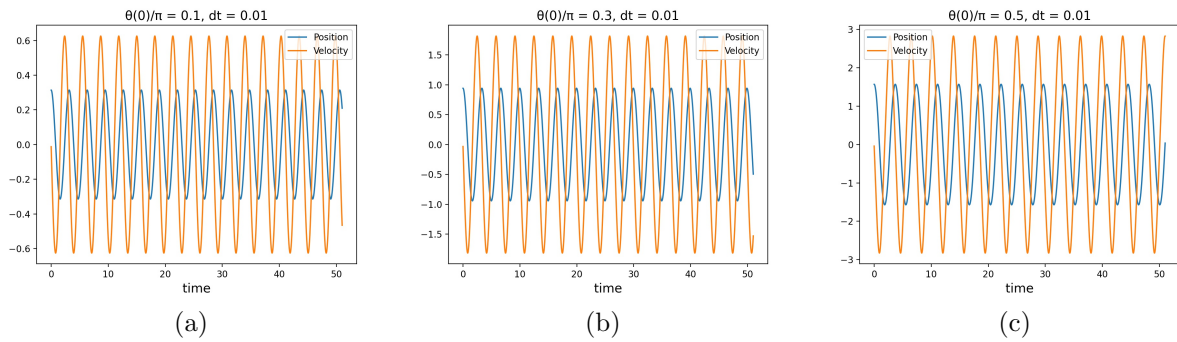


Figure 2: (a)  $\theta(0)/\pi = 0.1$ ; (b)  $\theta(0)/\pi = 0.3$ ; (c)  $\theta(0)/\pi = 0.5$

The simulated oscillations for the pendulum are at first glance identical to its harmonic counterpart. However, the period can be observed to be marginally shorter.

## Energy plots for the harmonic oscillator

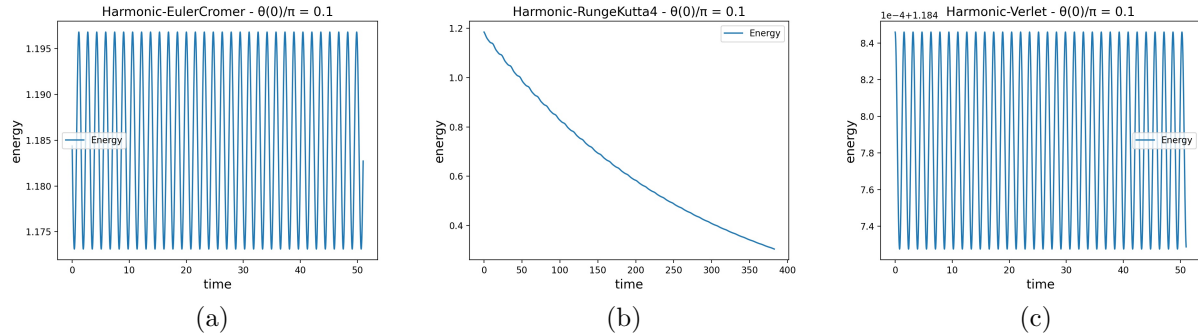


Figure 3: . (a) Euler Cromer; (b) Runge-Kutta; (c) Velocity Verlet

Initial conditions  $\theta(0)/\pi = 0.1$ ,  $\dot{\theta}(0) = 0$  and step size  $\Delta t = 0.01$  were utilized for the comparison. As can be observed, the energy plots for Euler-Cromer and Velocity Verlet are sinusoidal and predominately linear for Runge-Kutta. This implies that the latter is not energy-preserving and thus inferior as a numerical integrator. Compared to Velocity Verlet, a greater amplitude and thus energy discrepancy can be observed for Euler-Cromer. This is indicative of the satisfactory energy-preserving characteristics Velocity Verlet possesses, despite the higher order accuracy of Runge-Kutta.

## Energy plots for the pendulum

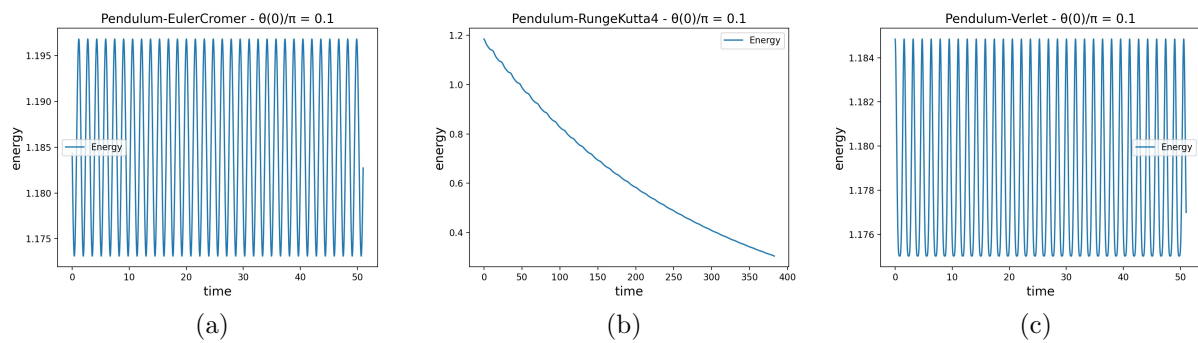


Figure 4: (a) Euler Cromer; (b) Runge-Kutta; (c) Velocity Verlet

The energy plots for the pendulum are similar compared to the harmonic oscillator, although Runge-Kutta demonstrates a more sinusoidal behavior with greater variance. It can also be noted that Velocity Verlet works inferiorly due to a much greater amplitude as compared to the harmonic oscillator.

## Comparison of different step sizes for Runge-Kutta

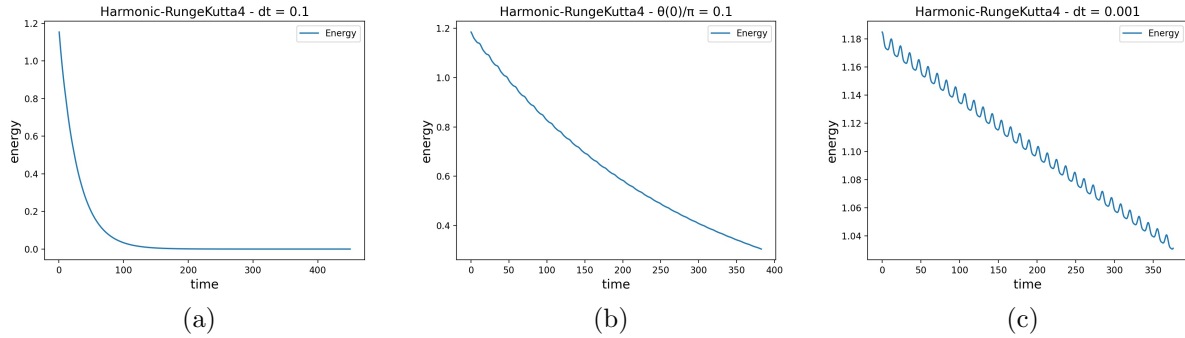


Figure 5: (a)  $\Delta t = 0.1$ ; (b)  $\Delta t = 0.01$ ; (c)  $\Delta t = 0.001$

In the order of 50 seconds, Runge-Kutta starts demonstrating a satisfactory linear behavior for a time step of  $\Delta t = 0.1$  and  $\Delta t = 0.01$  while becoming exponential for  $\Delta t = 0.1$ . Longer times require more marginal  $t$  in order to yield adequate results.

# Harmonic oscillator - Analytical and numerical solution

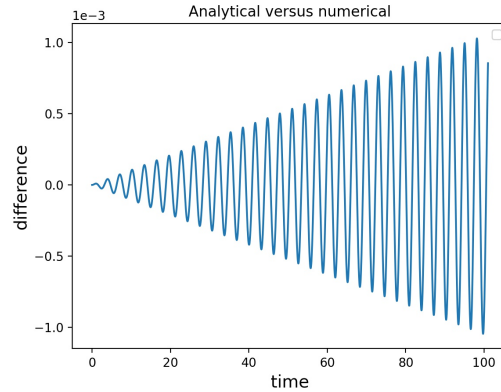


Figure 6

Using Verlet integration,  $\theta(0)/\pi = 0$  and  $\Delta t = 0.1$  the above-mentioned behavior are to be observed. The difference between the analytical and numerical solutions are calculated as:

$\text{analytical}(t) - \text{numerical}(t)$ ,

where:

$$\text{analytical}(t) = \theta(0)\pi \cdot \cos(\sqrt{g/l} \cdot t)$$

Since the discrepancy is within the order of  $10^{-3}$ , it can be concluded that the numerical solutions are of high precision.

## Project 1.2

### Comparison between the pendulum and perturbation series

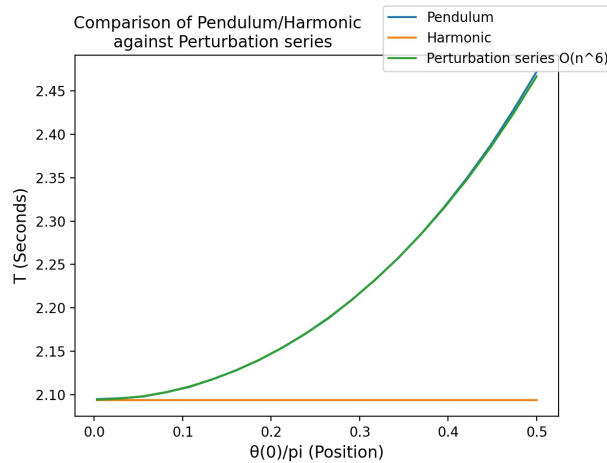


Figure 7

The sixth power of the perturbation series, i.e:

$$T = 2\pi \sqrt{\frac{l}{g}} \left( 1 + \frac{1}{16} \theta^2(0) + \frac{11}{3072} \theta^4(0) + \frac{173}{737280} \theta^6(0) \right),$$

sufficiently approximates the exponentially increasing period of the pendulum, while the period of the harmonic oscillator remains constant.

# Project 1.3

## The damped harmonic oscillator

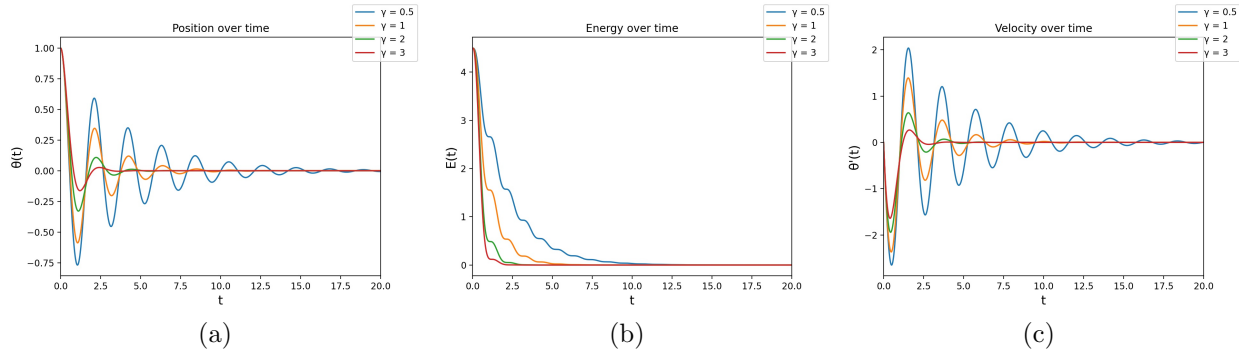


Figure 8: (a) Position over time; (b) Energy over time; (c) Velocity over time.

- Plot (a) Greater values for  $\gamma$  result in a decrease the relaxation time
- Plot (b) Energy decreases over time. Greater values for  $\gamma$  amplify the reduction speed.
- Plot (c) Greater values for  $\gamma$  result in a decrease of the relaxation time.  
It can also be noted that the velocity decreases over time.

## Relaxation time over $\gamma$

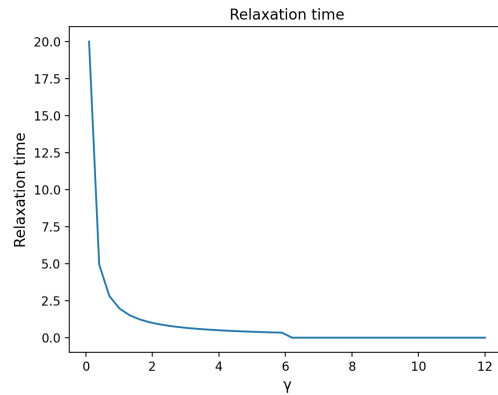


Figure 9

In order to determine the relaxation time, the vertices (local maxima) of the numerical solution were plotted and fitted with an exponential function in the form of:  $Ae^{-kt}$ . The relaxation time is subsequently calculated according to:  $T = \frac{1}{k}$ . At approximately  $\gamma \approx 5.9$ , critical dampening occurs, as that is the inflection point of the curve.

## Project 1.4

### Space phase portrait for the damped pendulum

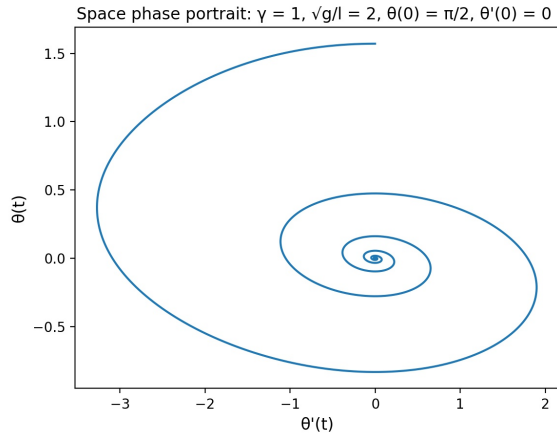


Figure 10

As  $\lim_{t \rightarrow \infty} \theta(t) = 0$  and  $\lim_{t \rightarrow \infty} \theta'(t) = 0$ , the spirals converge and the oscillations will eventually fade away.

# Project 1.5

## The double pendulum

Using the fourth order Runge-Kutta algorithm (with  $\Delta t = 0.003$ ), the generalized coordinates and momenta as function of time were plotted. Energies  $E = 1, 5, 10, 15$  and  $40$  were compared, with the specified initial values. The space phase diagrams of  $p_1$  versus  $q_1$  and  $p_2$  versus  $q_2$  were also plotted. Since the latter amalgamate the time plots into concise circular orbits, they are more useful in determining the nature of the trajectories. As such the space phase diagrams are utilized for this comparison.

Space phase diagrams for  $p_1$  versus  $q_1$

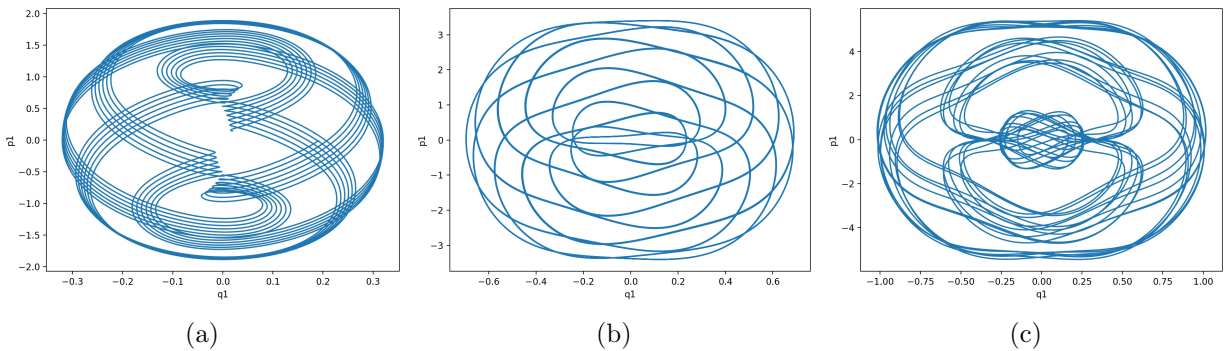


Figure 11: (a)  $E = 1$ ; (b)  $E = 5$ ; (c)  $E = 10$

Space phase diagrams for  $p_2$  versus  $q_2$

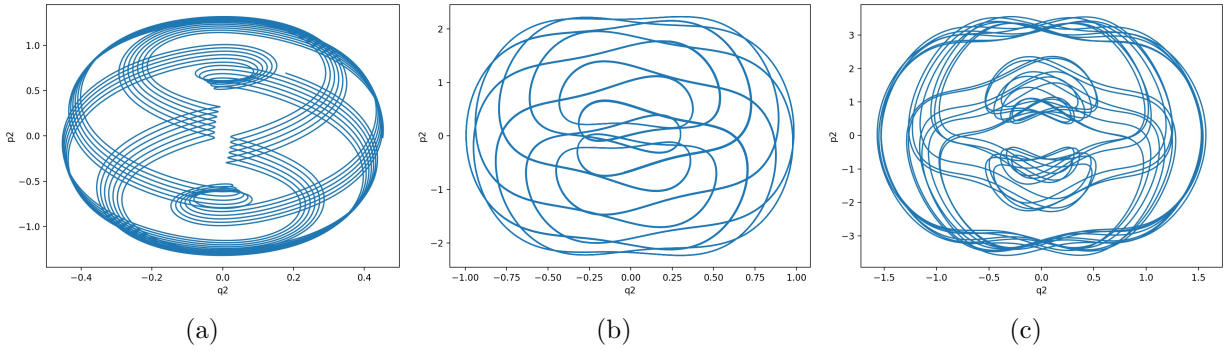


Figure 12: (a)  $E = 1$ ; (b)  $E = 5$ ; (c)  $E = 10$

### Space phase diagrams for $p_1$ versus $q_1$

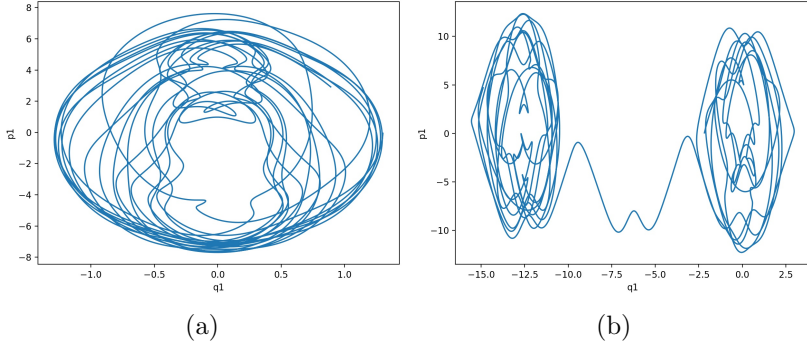


Figure 13: (a)  $E = 15$ ; (b)  $E = 40$ ;

### Space phase diagrams for $p_2$ versus $q_2$

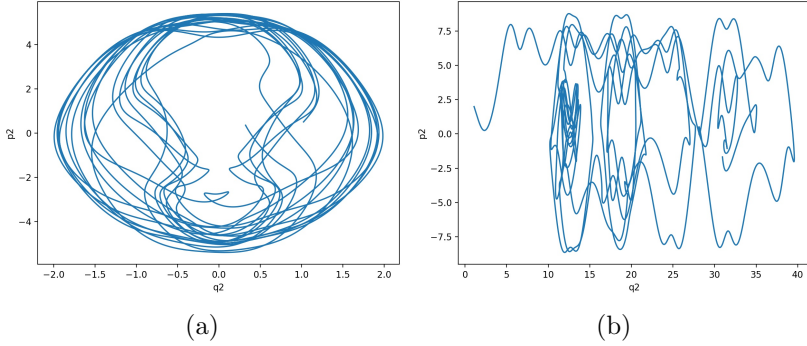


Figure 14: (a)  $E = 15$ ; (b)  $E = 40$ ;

As can be noted, the trajectories show a seemingly regular behavior for  $E = 1, 5, 10$ , but as  $E = 15$ , a more chaotic orbits are to be observed. For  $E = 40$ , a general pattern chaos is observed although its is more eminent in the  $p_2 - q_2$ -plot. I can thus be concluded that as  $E$  increases, regularity of the trajectories diminish while chaotic patterns start dominating. The critical value of the total energy at which some chaotic trajectories first occurs at  $E = 15$ .

It can also be concluded that for smaller angular initial conditions, i.e.  $q_1$  and  $q_2$ , more regular behavior are to be observed. Note that randomized angular initial conditions were generated for every simulation. However, several test runs for every energy concluded that the general pattern for chaos/regularity persists despite the different trajectories.

As for the Poincaré sections with initial conditions  $(q_1, q_2, p_1) = (0, 0, 0)$ , it can be concluded that for small values ( $E = 1 - 5$ ) the orbits appear seemingly regular. However, the orbits distorting from the regular elliptical paths for every energy level and becoming more scattered. However, all sections have strict reflection symmetry about  $q_1 = 0$  except for  $E = 40$  which will be discussed later.

### Poincaré sections for $E = 1, 5, 10$

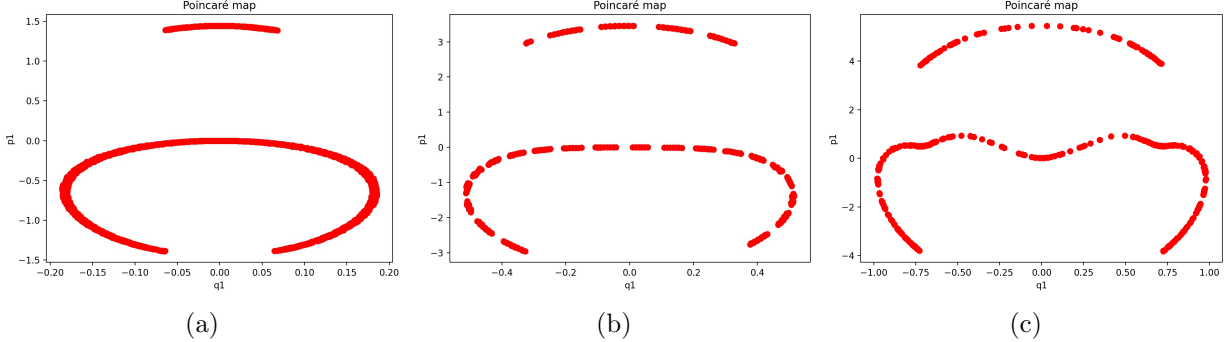


Figure 15: (a)  $E = 1$ ; (b)  $E = 15$ ; (c)  $E = 10$

### Poincaré sections for $E = 15, 40$

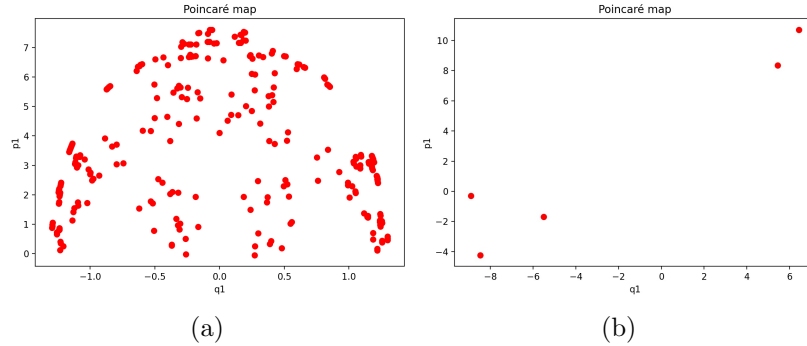


Figure 16: (a)  $E = 15$ ; (b)  $E = 40$ ;

For  $E = 15$ , the first appearance of chaos occurs and this plot is similar to that of figure 6.13 in *The chaotic motion of dynamical systems*. For  $E = 40$ , Poincaré sections become extremely sparse and thus chaotic. This is due to the fact that the energy for the pendulum is sufficient for the lower mass, but not the upper mass, to rotate. The rotational motion of the pendulum thus appears to be irregular for the observer.

For  $(q_1, q_2, p_1) = (1.1, 0, 0)$ , a similar behavior can be observed. However the Poincaré section for  $E = 15$  shows the same trend of distorted elliptical orbits, as in  $E = 1, 5, 10$  instead of the dense scatter plot as shown previously.